

## Conservative Circular Dichroism of Acridine Orange Bound to DNA

Toyoko IMAE and Shoichi IKEDA

*Department of Chemistry, Faculty of Science, Nagoya  
University, Nagoya, 464, Japan.*

(Received April 30, 1976)

**ABSTRACT:** The circular dichroism of acridine orange bound to DNA is calculated by the zeroth-order perturbation, based on the helical arrangements of bound dye. For the intercalation model, the Pritchard—Blake—Peacocke's arrangement of bound dye is assumed, in which a right-handed helix is formed along a polynucleotide chain. The nearest neighbor interaction is repulsive, and a conservative pair of circular dichroism bands having a positive band at the longer wavelength side appears, in agreement with the observation. It is found that two dye molecules intercalated at the adjacent sites produce the circular dichroism of the observed magnitude in the visible region. In the external association, dimeric dye molecules are bound to every other phosphate group on a polynucleotide chain, keeping their dye axes almost perpendicular to the helix axis and in its tangential direction. The nearest neighbor interaction is attractive, and a conservative pair of circular dichroism bands develops, having the opposite sign to the above; this agrees with the experimental result at very high binding ratios near unity. Calculations with the other models of both binding modes are also performed and the results are examined.

**KEY WORDS** Circular Dichroism / Acridine Orange / DNA /  
Intercalation / External Association / Dipole Strength / Rotatory  
Strength / Proflavine /

It has been known since the discovery of Neville and Bradley<sup>1</sup> that acridine orange acquires optical activity when it is combined with DNA in aqueous solution. In this connection and also from more physiological aspects, the modes of binding of acridine dye with DNA have been the principal interest of many investigators during the last decades,<sup>2,3</sup> and they have been examined by means of various methods, including measurements of absorption spectra, optical rotatory dispersion, and equilibrium dialysis.

There are two different modes of binding of aminoacridines with DNA, one strong and the other weaker.<sup>2,4,5</sup> Analysis of absorption spectra revealed that the strong binding process is associated with the binding of monomeric dye, and the weaker process with that of dimeric dye.<sup>2,3,5</sup> Various kinds of evidence have now established that the binding site of the monomeric

dye is located between two neighboring base pairs and the intercalation of monomeric dye occurs there.<sup>6-10</sup> Lerman<sup>6</sup> first showed by the X-ray diffraction of a proflavine—DNA complex that the intercalation of dye forces the separation of adjacent base pairs to increase. The intercalated aminoacridine has a molecular plane parallel to the base pairs, and the interplanar distance of acridine dye and base pair remains identical with that of the base pairs before intercalation occurs, *i.e.*, 3.40 Å. Lerman<sup>7</sup> put forward a model in which acridine dye is located above the hydrogen bonds formed between complementary bases.

Later studies<sup>11,12</sup> on the effects of denaturation of DNA showed, however, that the amount of intercalated dye did not decrease appreciably even when DNA was denatured. This was taken to mean that the bound dye molecule did not

interact with the two bases hydrogen-bonded to each other, but that it bound with two neighboring bases on the same polynucleotide chain, thus without untwisting the DNA double helix. Pritchard, *et al.*,<sup>13</sup> modified the intercalation model of Lerman in this way.

On the other hand, when the binding ratio is high or when the [P]/[D] (DNA phosphate/added dye) ratio is low, the dye molecule binds electrostatically with the polynucleotide chain through the ionized phosphate groups directed outside the double helix. This type of external binding was first postulated by Bradley and his coworkers.<sup>14,15</sup> The binding is much weaker and susceptible to the ionic strength. From spectral evidence it is known that the bound species interact strongly with one another and form aggregates mainly by the stacking interaction. The main binding species is identified as the dimeric dye molecule.

In this external association, the detailed mode of binding is not so clear as in the intercalation. From the measurements of electric dichroism, however, it is assumed that the longer axis of the dye molecular plane lies nearly perpendicular to the helix axis.<sup>3,16</sup>

In both modes of binding, *i.e.*, intercalation and external association, characteristic circular dichroism is induced on the bound acridine dye. This is seen in the extrinsic circular dichroism of the visible absorption region of the dye, which varies with the binding ratio or the [P]/[D] ratio.<sup>3,17</sup>

In both models of binding presented above, a helical array of bound dye molecules can be formed, compatible with the geometry of DNA helix, and it can form an exciton. The optical rotatory power of such a helical array of acridine dye can be calculated by means of the Moffitt—Fitts—Kirkwood—Tinoco theory.<sup>18</sup> In the present work the zeroth-order perturbation treatment of optical activity will be applied to the helical arrays of acridine orange on DNA, without paying attention to the first order perturbation arising from the electronic coupling of the bound dye with the base pair and of the externally bound dye with the intercalated dye. Two electronic transitions of acridine orange are considered, one around 500 nm and the other at 260 nm,<sup>19,20</sup> although the latter transition overlaps

with that of the DNA bases.

## THEORETICAL

When  $N$  identical chromophores are coupled electronically through the formation of a regular helical array, each excited state of the chromophore splits into  $N$  exciton levels.<sup>21,22</sup> The dipole strength and the rotatory strength associated with a transition from the ground state to the  $K$ -th level of an excited state,  $E$ , can be calculated by<sup>18</sup>

$$D_{EK} = \mu_{0e,\parallel}^2 \left\{ 1 + \sum_k \sum_{l \neq k}' C_{keK} C_{leK} \right\} + \mu_{0e,\perp}^2 \left\{ 1 + \sum_k \sum_{l \neq k}' C_{keK} C_{leK} \cos \frac{2\pi}{P}(l-k) \right\} = \frac{1}{3} D_{EK,\parallel} + \frac{2}{3} D_{EK,\perp} \quad (1)$$

and

$$R_{EK} = \frac{\pi \nu_{E0}}{c} a \mu_{0e,\parallel} \mu_{0e,t} \sum_k \sum_{l \neq k}' C_{keK} C_{leK} \times \left\{ 1 - \cos \frac{2\pi}{P}(l-k) \right\} - \frac{\pi \nu_{E0}}{2c} b \mu_{0e,\perp}^2 \sum_k \sum_{l \neq k}' (l-k) \times C_{keK} C_{leK} \sin \frac{2\pi}{P}(l-k) \quad (2)$$

respectively, where  $c$  is the velocity of light,  $a$  and  $b$  are the radius and the pitch per chromophore of the helix of chromophores, and  $P$  is

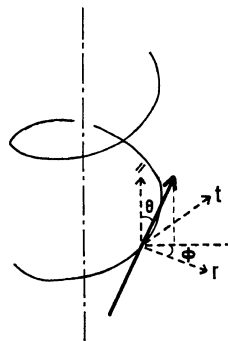


**Figure 1.** Direction of transition moments in a right-handed helical array. The parallel component ( $\mu_{\parallel}$ ) is directed to the helix axis, and the perpendicular component decomposes into radial ( $r$ ) and tangential ( $t$ ) components.

the number of chromophores per helical turn. Here  $\nu_{E0}$  is the unperturbed frequency, and  $\mu_{0e}$  is the transition electric moment of chromophore, with suffices, //, t, and  $\perp$  representing the parallel, tangential, and perpendicular components. As shown in Figure 1, the parallel and tangential directions are taken in accord with the helix-advancing direction. The angles  $\theta$  and  $\phi$  defining the direction of the transition moment are also given in Figure 1. The coefficient  $C_{keK}$  is obtained from a set of linear equations

$$\sum_{k=1}^N (V_{k0e,10e} - \delta_{k,l} E'_{EK}) C_{keK} = 0, \quad l=1, 2, \dots, N \quad (3)$$

and orthonormal conditions

$$\sum_{K=1}^N C_{keK} C_{leK} = \delta_{k,l} \quad (4)$$

where  $V_{k0e,10e}$  is the dipole-dipole interaction potential between the  $k$ -th and  $l$ -th chromophores,  $E'_{EK}$  is the perturbed energy, and  $\delta_{k,l}$  is the Kronecker's delta. The frequency of the transition associated with the  $K$ -th level is given by

$$\begin{aligned} \nu_{EK} &= \nu_{E0} + \frac{E'_{EK}}{h} \\ &= \nu_{E0} + \frac{1}{h} \sum_k \sum_{l \neq k} C_{keK} C_{leK} V_{k0e,10e} \end{aligned} \quad (5)$$

where  $h$  is Planck's constant.

Rotatory strength is associated with all the exciton levels, so that every level has its own circular dichroism. If the circular dichroism has a common band shape,  $f(\nu - \nu_{EK})$ , centered at  $\nu_{EK}$ , the observable molar ellipticity per chromophore is the sum of all these bands, that is, it is given by

$$[\theta]_E = \frac{48\pi^2 N_A}{Nhc} \nu \sum_{K=1}^N R_{EK} f(\nu - \nu_{EK}) \quad (6)$$

where  $N_A$  is Avogadro's number.

It is found that eq 6 gives a conservative pair of positive and negative circular dichroism bands for the present systems. To discriminate simply the sign of the pair of circular dichroism bands, that is, to see which band, positive or negative, is at the longer wavelength side, it is more convenient to expand eq 6 around  $\nu - \nu_{E0}$ . The zeroth-order approximation gives a pair of bands expressed by

$$[\theta]_E = -\frac{48\pi^2 N_A}{Nhc} \nu \sum_{K=1}^N (\nu_{EK} - \nu_{E0}) R_{EK} \frac{\partial f(\nu - \nu_{E0})}{\partial \nu} \quad (7)$$

and the sign of the pair is determined by the rotatory oscillator strength term

$$\begin{aligned} &\sum_{K=1}^N (\nu_{EK} - \nu_{E0}) R_{EK} \\ &= \frac{\pi \nu_{E0}}{hc} a \mu_{0e, //} \mu_{0e, t} \sum_k \sum_{l \neq k}' V_{k0e,10e} \\ &\quad \times \left\{ 1 - \cos \frac{2\pi}{P} (l-k) \right\} \\ &\quad - \frac{\pi \nu_{E0}}{2hc} b \mu_{0e, \perp}^2 \sum_k \sum_{l \neq k}' (l-k) \\ &\quad \times V_{k0e,10e} \sin \frac{2\pi}{P} (l-k) \end{aligned} \quad (8)$$

For a helical array of chromophores, each directing its transition moment perpendicular to the helix axis, the first term of eq 8 vanishes. If the interaction potential between the nearest neighbors is much stronger than those between any others, the sign of the rotatory oscillator strength term is chiefly determined by the sign of  $V_{10e,20e} \sin 2\pi/P$ . For helices having  $P > 2$ , the sign of the conservative band is then determined by the sign of  $V_{10e,20e}$ . If the nearest neighbor potential is repulsive, a positive band of the pair appears at the longer wavelength side; if it is attractive, a negative band appears at the longer wavelength side.

If the band shape is Gaussian with the half width  $\Theta_E$ , it is written

$$f(\nu - \nu_{EK}) = \frac{1}{\Theta_E \sqrt{\pi}} \exp[-\{(\nu - \nu_{EK})/\Theta_E\}^2] \quad (9)$$

In the following, values of spectral strengths,  $D_{EK}/N$  and  $R_{EK}/N$ , are given in the unit of chromophore, either monomeric or dimeric, depending on the modes of binding, and values of molar ellipticity,  $[\theta]$ , are expressed on the molar basis of the bound dye.

## STRUCTURE OF THE COMPLEXES AND THEIR MODELS

### *Intercalation Model*

In aqueous solution the native DNA has a B-form conformation, which consists of a right-

handed double helix having the molecular plane of base pairs perpendicular to the helix axis. The number of base pairs per helical turn is 10 and the repeat distance of a residue along the helix axis is 3.40 Å. In the intercalation model of Pritchard—Blake—Peacocke,<sup>13</sup> acridine dye molecules bind with a polynucleotide chain by the stacking force. If the intercalation occurs at consecutive sites along the DNA helix, the bound dye molecules are arranged in a helical way along one of the polynucleotide chains. The formation of a sequence of bound dye, that is, the intercalation of dye adjacent to the site already intercalated, could occur, since the occupied site and its neighbors would be more or less subject to the structural perturbation.

The visible transition of acridine dye has an electric moment parallel to the longer axis of the molecular plane.<sup>20</sup> Then the transition moment of the intercalated dye is perpendicular to the helix axis:  $\theta=90^\circ$ . It was rather arbitrarily put perpendicular to the radial direction of helix:  $\phi=90^\circ$ . Since the dye intercalated between base pairs increases their separation, without twisting the DNA helix, its repeat distance along the helix is equal to 6.80 Å and the number of chromophore per turn is 10. In the present model based on the Pritchard—Blake—Peacocke model, the central pyridine ring of bound dye was located above the pyrimidine ring or pentacyclic ring of purine, and the distance of the transition moment from the helix axis was put equal to 4.00 Å.

To obtain values of electronic parameters for the visible transition, the spectral data of the acridine orange—DNA system observed at high [P]/[D] ratios were examined, in which the intercalated dye monomer was thought to be free from the electronic coupling with the other bound dye. Fredericq and Houssier<sup>3</sup> assumed that this condition was fulfilled at [P]/[D] higher than 20. Consequently, the frequency and area of the absorption band obtained at [P]/[D] 200, *i.e.*, at the binding ratio 0.005 in 0.001-*M* NaCl, were taken for this purpose. The observed absorption band was not symmetrical, but its half-width was assumed to be 1725  $\text{cm}^{-1}$  as if it were Gaussian.

The ultraviolet transition of acridine orange is also polarized in the same direction as the

Table I. Geometrical parameters for the transition moment

	$a$ , Å	$b$ , Å	$P$	$\theta$ , deg	$\phi$ , deg
Intercalation	4.00	6.80	10	90	90
External binding	12.00	6.80	5	80	90

Table II. Electronic parameters for the visible and ultraviolet transition

	E	$\frac{c}{\nu_{E0}}$ , nm	$\mu_{0e}$ , D	$\frac{\theta_E}{c}$ , $\text{cm}^{-1}$
Intercalated monomer	A	505	7.31	1725
	B	261	8.16	3400
Externally bound dimer	A	458	7.12	1725
	B	261	7.98	3400

visible transition.<sup>20</sup> However, values of electronic parameters for the transition can not be obtained experimentally, since the base pair also absorbs the same spectral region. They were simply assumed with reference to those obtained for the acridine orange—polypeptide systems.<sup>23,24</sup>

The numerical values of the geometrical and electronic parameters are summarized in Tables I and II.

#### External Association Model

The unit of externally bound dye is assumed to be a dimeric dye, the structure of which is an antiparallel stacked arrangement of two molecules, as proposed by Zanker.<sup>19,25</sup> The dimeric dye molecules bind with phosphate groups electrostatically, and the bound molecules strongly interact with one another so that they form a polymeric array along the DNA helix. The longer axis of the molecular plane of the bound dye is known to be almost perpendicular to the helix axis of DNA. It was arbitrarily tilted by  $10^\circ$  from being perpendicular to the helix axis. The effect of this tilt was examined, as will be shown later. In such arrangements of dimeric dye, consideration of steric hindrance and the stacking tendency of the dye would lead to the structure in which every other phosphate group on one of the two polynucleotide chains is a binding site forming a helical sequence. The repeat distance of dimeric dyes along the helix

axis is then 6.80 Å, and the number of chromophores per turn is 5.

The direction of the transition moment in concern remains to be parallel to the longer axis of the dye molecular plane for the assumed dimer structure. Consequently, the transition moment tilts from perpendicular to the helix axis by  $10^\circ$ :  $\theta=80^\circ$ . It was located at 12.00 Å from the helix axis and put perpendicular to the radial direction:  $\phi=90^\circ$ . The extension of the DNA helix around the externally bound sites is not considered.

Values of the electronic parameters of the visible transition for the external association model were taken from the absorption spectra observed at a low  $[P]/[D]$  ratio, 0.6, or at the binding ratio of approximately unity in 0.001-*M* NaCl.<sup>3</sup>

Table I gives values of the geometrical parameters, and Table II lists values of the electronic parameters used for both visible and ultraviolet transitions.<sup>23,24</sup>

## RESULTS AND DISCUSSION

### Intercalation Model

Since the intercalated dye molecules have their longer axes perpendicular to the helix axis, the expressions for spectral strengths reduce to simpler forms. In the present model, it is clear that the dipole-dipole interaction potential between intercalated dye molecules is the strongest and repulsive for the nearest neighbors. Then eq 8 gives a negative value for the rotatory oscillator strength term, and, consequently, eq 7 yields a conservative pair having a positive band at the longer wavelength side and a negative band at the shorter wavelength side. This is in agreement with the observations.

Actual calculation of the potential leads to a value for the nearest neighbors more than 35 times larger than that for any others. Dipole strength and rotatory strength were calculated by eq 1 and 2 for different numbers of dye molecules,  $N$ , in a helical sequence, and the results for the visible bands are given in Figure 2. There are two significant dipole strengths, which shift to the blue with increasing  $N$ . Two or more rotatory strengths have appreciable magnitudes, positive at the longer wavelength

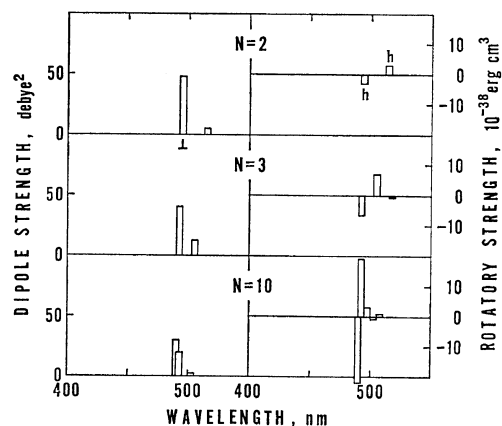


Figure 2. Calculated spectral strengths of intercalated acridine orange for the visible transition.  $N$  is the number of intercalated monomeric dyes.  $\perp$  denotes the perpendicular component, and  $h$  denotes the contribution of the helical term or pitch-dependent term, *i.e.*, the second term of eq 2.

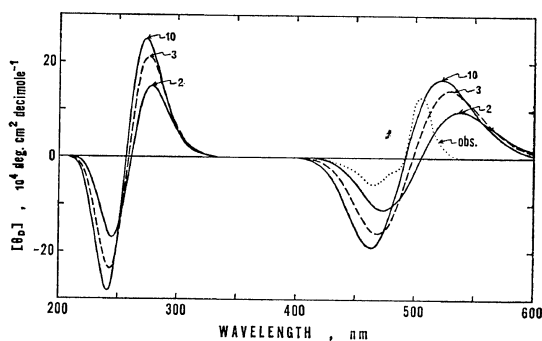


Figure 3. Circular dichroism of acridine orange intercalated to DNA: —, calculated for different numbers of dyes,  $N$ ; ---, observed for  $[P]/[D]$  5 in 0.001-*M* NaCl, pH 6–6.5,  $[D]=1.0 \times 10^{-5}$  *M*.

side and negative at the shorter wavelength side, and a conservative pair is formed, as predicted above.

Figure 3 shows the calculated circular dichroism in the visible and ultraviolet regions. For comparison, the observed spectrum was quoted from the results obtained with acridine orange bound to calf thymus DNA at  $[P]/[D]$  5 in 0.001-*M* NaCl.<sup>3</sup> It has a positive band at 505 nm, a negative band at 465 nm, and a negative shoulder at 482 nm. The negative shoulder would have arisen from the mixing of a negative band at

**Table III.** Visible rotatory strengths and molar ellipticity calculated for various intercalation models of  $N=2$ 

Mode of binding	Modification from Table I	$\frac{V_{10a,20a}}{hc}$ , cm <sup>-1</sup>	$\frac{c}{\nu}$ , nm	$\frac{R_{AK}}{N}$ , DBM	$\frac{c}{\nu}$ , nm	$[\theta]$
Present		349	514 496	3.58 -3.58	540 475	98,000 -111,000
Lerman <sup>7</sup>	$\begin{cases} a=2.00 \text{ \AA} \\ \phi=115^\circ \end{cases}$	603	521 490	3.58 -3.58	540 475	160,000 -182,000
Armstrong, <i>et al.</i> <sup>5</sup>	$b=10.20 \text{ \AA}$	153	509 501	5.37 -5.37	535 475	66,000 -75,000
Modified Gardner—Mason <sup>28</sup>	$\theta=93^\circ$	413	516 495	3.64 -3.64	540 475	116,000 -132,000

475 nm, observed with the solutions of lower  $[P]/[D]$ , in which external association occurred.

The calculated spectra do not necessarily coincide with that observed, especially in the band position, but consideration of nonconservative contributions,<sup>24</sup> which arise mainly from the coupling with DNA bases in contact and will be found to be positive, would shift the positive band to the blue and make the spectrum for  $N=2$  comparable with the observed one. Thus it may be concluded that two monomeric dye molecules intercalated in the adjacent sites produce the observed circular dichroism. This result is compatible with the observation of Fredericq and Houssier<sup>3</sup> that the rotatory strength varies with the square of the binding ratio. It does not support, however, the postulate of Armstrong, *et al.*,<sup>5</sup> that the sites immediately adjacent to those occupied must be vacant, as can be seen more clearly below.

Table III summarizes the numerical results calculated for some intercalation models of  $N=2$  with different geometrical parameters.

It is noted that the values of the rotatory strength for any intercalation model do not change very much from those for the above, as long as the transition moments are aligned perpendicular to the helix axis. This can be expected from the treatment of the nearest neighbor approximation, which gives an expression for the exciton coefficients  $C_{keK}$  independent of the interaction potential.<sup>26</sup> However, the frequency depends on the magnitude of interaction, and the resulting circular dichroism varies from that given above. Lerman's model<sup>7</sup> and that of

Armstrong, *et al.*,<sup>5</sup> belong to this category, as given in Table III.

In the Lerman model the dye axis is put parallel to and just above the hydrogen bonds of the guanine—cytosine base pairs;<sup>7</sup> a similar mode of binding would hold for adenine—thymine base pairs as well.<sup>13</sup> For the dye intercalated closer to the helix axis, the calculated circular dichroism is too strong. When the intercalation occurs at alternate sites, as in the postulate of Armstrong, *et al.*,<sup>5</sup> the repeat distance of the dye increases by a one and a half, and the rotatory strength increases by just that factor. The resulting circular dichroism is much weaker owing to the weaker interaction.

Mason and McCaffery<sup>27</sup> measured the flow circular dichroism of an aqueous solution of acridine orange complexed with DNA; they suggested that the longer axes of the bound dye molecules should tilt from being perpendicular to the helix axis. They assigned the positive band at 505 nm as the perpendicular component and the negative band at 467 nm as the parallel component. Then the first term of eq 2, the radius-dependent term, must make a significant contribution; also, to make the sign of the bands in agreement with the observation, the dye axis must be tilted in such a way that  $\mu_{0a, \parallel} \mu_{0a, \perp} < 0$ . Such a tilt of bound dye molecules can be obtained by stretching the B-form DNA double helix in the direction of its axis.

While Gardner and Mason<sup>28</sup> proposed an intercalation model in which all the base pairs of DNA were also slightly tilted from being perpendicular to the helix axis, the present calculation

## Calculation of Extrinsic Circular Dichroism

**Table IV.** Visible rotatory strengths and molar ellipticity calculated for various external association models of  $N=10$ 

Mode of binding	Modification from Tables I and II	$\frac{V_{10a,20a}}{hc}$ , cm <sup>-1</sup>	The two strong strengths			[ $\theta$ ]
			$\frac{c}{\nu}$ , nm	$\frac{R_{AK}}{N}$ , DBM	$\frac{c}{\nu}$ , nm	
Present		-104	459	-21.24	480	-23,000
			458	12.82	430	26,000
Present	$\theta=90^\circ$	-85.6	459	-18.87	485	-42,000
			458	16.04	435	47,000
Present	$\theta=100^\circ$	-60.4	458.4	-15.83	485	-45,000
			457.8	17.66	435	50,000
(1-2) Binding	$\theta=75^\circ$	-188	467	25.05	500	56,000
(1-4') Binding	$b=3.40 \text{ \AA}, P=10$ $\theta=150^\circ$	732	440	13.91	460	337,000
			427	-27.86	410	-382,000
Monomer Binding	$b=3.40 \text{ \AA}, P=10$ $\frac{c}{\nu_{A0}}=492 \text{ nm}$ $\mu_{0a}=7.31 \text{ D}$	-864	532	-12.12	555	-173,000
			519	6.81	490	190,000

was carried out on a model in which only the dye axes were tilted by  $3^\circ$  in such a way as to satisfy the above requirement; this is given in Table III. The calculated circular dichroism agrees with that observed and is also consistent with the observation under flow conditions.

Proflavine intercalates into DNA similarly to acridine orange, since the binding constants for the intercalation of both dyes are the same.<sup>5</sup> The circular dichroism induced on bound proflavine is, however, lower.<sup>29,30</sup> This would be attributable to a lower value of the transition moment of the intercalated dye, as revealed in its absorption spectra.<sup>5,10,31</sup>

#### External Association Model

At first, the externally associated dye molecules are set with their longer axes perpendicular to the helix axis. The dipole-dipole interaction is the strongest for the nearest neighbors; actual calculation yields a negative value more than six times larger in magnitude than the others. Numerical values are given in Table IV. The attraction makes eq 8 positive, and a negative circular dichroism band appears at the longer wavelength side and a positive band at the shorter wavelength side. This is in agreement with the result observed. However, the observed spectrum was found to be of the same order

of magnitude as that calculated for  $N=2$  or  $3$ , and this number of aggregation is too small when compared with the binding ratio of about unity.

Fredericq and Houssier<sup>3</sup> claimed that the dye axes are not necessarily strictly perpendicular to the helix axis but their arrangement departs somewhat from perpendicularity. Based on this suggestion, calculations were carried out by tilting the dye axes by  $\pm 10^\circ$  from the perpendicular to the helix axis.

For  $\theta=100^\circ$ , the interaction potential becomes weaker for the nearest neighbors, but the first term of eq 2 contributes to increase the magnitude of rotatory strength. The resulting circular dichroism remains almost the same as for  $\theta=90^\circ$ , as shown in Table IV; it is too strong for a given sequence length.

On the other hand, for  $\theta=80^\circ$ , the interaction potential is stronger, but the first term of eq 2 contributes oppositely to the second term, reducing the magnitude of the rotatory strength. Figure 4 shows calculated distributions of dipole strengths and rotatory strengths for the visible transition. Figure 5 gives the calculated circular dichroism and compares it with the observed one for the binding ratio  $\approx 1$  or at  $[P]/[D]$  0.6 in 0.001-*M* NaCl.<sup>3</sup> The calculated curve for

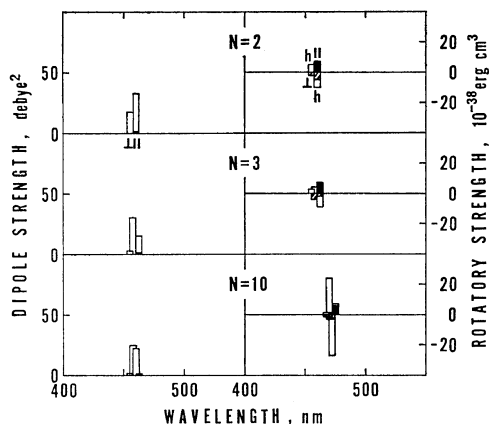


**Figure 4.** Calculated spectral strengths of externally associated acridine orange for the visible transition.  $N$  is the number of bound dimeric dyes. Left,  $D_{AK}/N$ : Solid bar, the first term of eq 1, i.e.,  $D_{AK, \parallel}/3N$ ; open bar, the second term of eq 1, i.e.,  $2D_{AK, \perp}/3N$ . Right,  $R_{AK}/N$ : Solid, hatched, and open bars represent the first ( $\parallel$ ), second ( $\perp$ ), and third ( $h$ ) terms of eq 2 modified as follows:

$$R_{AK} = \frac{\pi \nu_{A0}}{3c} a \mu_{0a, \parallel} \mu_{0a, \perp} \left( \frac{D_{AK, \parallel}}{\mu_{0a, \parallel}^2} - \frac{2D_{AK, \perp}}{\mu_{0a, \perp}^2} \right) + \frac{1}{3} R_{AK}^{\parallel}$$

$N=10$  is comparable with the observed one. The latter has a negative band at 475 nm and a positive band at 440 nm. Nonconservative circular dichroism would improve the agreement,<sup>24</sup> since it will come from the coupling with the ultraviolet transitions of the stacked dimeric dye and of the DNA bases and will be found to be negative. Thus it can be concluded that a long helical sequence of externally bound dimeric dye must be formed to induce the observed circular dichroism. Armstrong, *et al.*,<sup>5</sup> postulated that the bound 'dimer' is formed by fixation of the monomer to that already intercalated. Owing to the smaller radius, the interaction would be stronger and the circular dichroism would be too strong with their model.

It is worth considering possible sites for the external binding of diaminoacridines. In the electrostatic interaction of dye with DNA, the phosphate groups must play a central role. For the assumed helical radius, 12.00 Å, the neighboring phosphate groups on the same polynucleotide chain are 8.2 Å apart, which fits to the

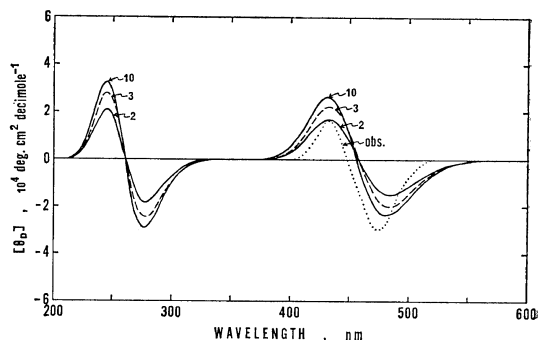


**Figure 5.** Circular dichroism of acridine orange externally bound to DNA: —, calculated for different numbers of dimeric dyes,  $N$ ; ---, observed for  $[P]/[D]$  0.6 in 0.001- $M$  NaCl, pH 6–6.5,  $[D]=1.0 \times 10^{-5} M$ .

dimethylamino groups of acridine orange with the least difficulty. In this model, called the (1–2) binding in Table IV, the tilt of the dye axis becomes larger;  $\theta=75^\circ$ . This increase in tilt gives rise to a considerable magnitude of the first term of eq 2 and to a change in sign of the conservative pair of circular dichroism bands. Such a result conflicts with the experimental one.

The other possible sites must be phosphate groups of the third neighbors but on another polynucleotide chain, which are 10.5 Å apart and can fit with acridine orange. This model is designated as the (1–4') binding. Using values given in Table IV for the parameters, the nearest neighbor interaction is repulsive, and the calculated circular dichroism is found to have the opposite signs to those observed.

Since phosphate groups of all the other pairs are farther apart and are not compatible with acridine dye, any model consisting of electrostatic binding at two sites must be abandoned. In addition to the electrostatic binding at one site, another interaction must be operative to keep the longer axes of the externally associated dye nearly perpendicular to the helix axis. Such an interaction of externally bound dye could occur with either the base pair of DNA or the already intercalated dye. The former is preferable for the present model, although the latter was postulated by Armstrong, *et al.*,<sup>5</sup> at least, in the initiation of external binding.



It has been usual to assign the monomeric dye at the unit for external binding. If this were true, however, the circular dichroism would appear red-shifted by about 70 nm, as shown in Table IV. Thus the binding mechanism of monomeric dye must be excluded.

Proflavine has weaker stacking tendency than acridine orange.<sup>32</sup> It binds externally with DNA to a less extent<sup>5</sup> and interacts less strongly with one another. Furthermore, it was assumed that weakly bound proflavine does not contribute to optical rotation.<sup>33</sup>

Finally it is pertinent to refer to a calculation of the optical rotatory dispersion of the acridine orange—DNA complex, performed by Tinoco, *et al.*<sup>18</sup> They calculated the nearest neighbor interaction potential<sup>26,34</sup> by putting the transition moments for the monomeric dye outside the DNA helix. Since they assumed  $\theta=90^\circ$  but  $\phi=0^\circ$ , *i.e.*,  $\mu_{0a,t}=0$ , instead of  $\phi=90^\circ$  in the present model of external association, they obtained a positive value for the interaction, unlike the present model. They drew rotatory dispersion curves having the sign of Cotton effects coincident with that of the observed one, based on the double-stranded helix model. However, the observed rotatory dispersion<sup>1</sup> would possibly be for the intercalated dye, which exhibited Cotton effects with signs opposite to those for the externally associated dye.

## REFERENCES

1. D. M. Neville, Jr., and D. F. Bradley, *Biochim. Biophys. Acta*, **50**, 397 (1961).
2. A. Blake and A. R. Peacocke, *Biopolymers*, **6**, 1225 (1968).
3. E. Fredericq and C. Houssier, *ibid.*, **11**, 2281 (1972).
4. A. R. Peacocke and J. N. H. Skerrett, *Trans. Faraday Soc.*, **52**, 261 (1956).
5. R. W. Armstrong, T. Kurucsev, and U. P. Strauss, *J. Amer. Chem. Soc.*, **92**, 3174 (1970).
6. L. S. Lerman, *J. Mol. Biol.*, **3**, 18 (1961).
7. L. S. Lerman, *J. Cell. Comp. Physiol.*, **64**, 1 (1964).
8. Y. Mauss, J. Chambron, M. Daune, and H. Benoit, *J. Mol. Biol.*, **27**, 579 (1967).
9. V. Luzzati, F. Masson, and L. S. Lerman, *ibid.*, **3**, 634 (1961).
10. D. M. Neville, Jr., and D. R. Davies, *ibid.*, **17**, 57 (1966).
11. D. S. Drummond, V. F. W. Simpson-Gildemeister, and A. R. Peacocke, *Biopolymers*, **3**, 135 (1965).
12. M. Liersch and G. Hartmann, *Biochem. Z.*, **343**, 16 (1965).
13. N. J. Pritchard, A. Blake, and A. R. Peacocke, *Nature*, **212**, 1360 (1966).
14. D. F. Bradley and M. K. Wolf, *Proc. Nat. Acad. Sci.*, **45**, 944 (1959).
15. A. L. Stone and D. F. Bradley, *J. Amer. Chem. Soc.*, **83**, 3627 (1961).
16. D. F. Bradley, N. C. Stellwagen, C. T. O'Konski, and C. M. Paulson, *Biopolymers*, **11**, 645 (1972).
17. M. Zama and S. Ichimura, *ibid.*, **9**, 53 (1970).
18. I. Tinoco, Jr., R. W. Woody, and D. F. Bradley, *J. Chem. Phys.*, **38**, 1317 (1963); I. Tinoco, Jr., *J. Amer. Chem. Soc.*, **86**, 297 (1964).
19. V. Zanker, *Z. Phys. Chem.*, **199**, 225 (1952).
20. V. Zanker, *ibid.*, *N. F.*, **2**, 52 (1954).
21. W. Moffitt, *J. Chem. Phys.*, **25**, 467 (1956).
22. W. Moffitt, D. D. Fitts, and J. G. Kirkwood, *Proc. Nat. Acad. Sci.*, **43**, 723 (1957).
23. S. Ikeda and T. Imae, *Polymer J.*, **4**, 301 (1973).
24. T. Imae and S. Ikeda, *Biopolymers*, **15**, 1655 (1976).
25. R. E. Ballard and C. H. Park, *J. Chem. Soc.*, **A1970**, 1340.
26. D. F. Bradley, I. Tinoco, Jr., and R. W. Woody, *Biopolymers*, **1**, 239 (1963).
27. S. F. Mason and A. J. McCaffery, *Nature*, **204**, 468 (1964).
28. B. J. Gardner and S. F. Mason, *Biopolymers*, **5**, 79 (1968).
29. H. J. Li and D. M. Crothers, *ibid.*, **8**, 217 (1969).
30. D. G. Dalgleish, H. Fujita, and A. R. Peacocke, *ibid.*, **8**, 633 (1969).
31. K. Yamaoka, *ibid.*, **11**, 2537 (1972).
32. G. R. Haugen and W. H. Melhuish, *Trans. Faraday Soc.*, **60**, 386 (1964).
33. A. Blake and A. R. Peacocke, *Biopolymers*, **4**, 1091 (1966).
34. D. F. Bradley, S. Lifson, and B. Honig in "Electronic Aspects in Biochemistry," B. Pullman, Ed., Academic Press, London, 1964, p 77.